



THE UNIVERSITY *of* EDINBURGH

Edinburgh Research Explorer

Detrital cosmogenic ^{21}Ne records decoupling of source to sink signals by sediment storage and recycling in Miocene to present rivers of the Great Plains

Citation for published version:

Sinclair, H, Stuart, FM, Mudd, S, McCann, L & Tao, Z 2018, 'Detrital cosmogenic ^{21}Ne records decoupling of source to sink signals by sediment storage and recycling in Miocene to present rivers of the Great Plains', *Geology*, vol. 47, no. 1, pp. 3-6. <https://doi.org/10.1130/G45391.1>

Digital Object Identifier (DOI):

[10.1130/G45391.1](https://doi.org/10.1130/G45391.1)

Link:

[Link to publication record in Edinburgh Research Explorer](#)

Document Version:

Peer reviewed version

Published In:

Geology

General rights

Copyright for the publications made accessible via the Edinburgh Research Explorer is retained by the author(s) and / or other copyright owners and it is a condition of accessing these publications that users recognise and abide by the legal requirements associated with these rights.

Take down policy

The University of Edinburgh has made every reasonable effort to ensure that Edinburgh Research Explorer content complies with UK legislation. If you believe that the public display of this file breaches copyright please contact openaccess@ed.ac.uk providing details, and we will remove access to the work immediately and investigate your claim.



1 Detrital cosmogenic ^{21}Ne records decoupling of source to
2 sink signals by sediment storage and recycling in Miocene
3 to present rivers of the Great Plains

4 H.D. Sinclair¹, F.M. Stuart², S.M. Mudd¹, L. McCann^{1,2}, and Z. Tao^{1,2}

5 ¹*School of GeoSciences, University of Edinburgh, Edinburgh EH8 9XP, UK*

6 ²*Isotope Geosciences Unit, Scottish Universities Environmental Research Centre, East
7 Kilbride G75 0QF, UK*

8 **ABSTRACT**

9 The preservation of conglomerates far from mountainous sources are commonly
10 interpreted in terms of tectonic or climatic forcing. To relate a depositional signal to
11 changing conditions in source areas, the process and duration of sediment routing from
12 source to sink need to be determined. For the first time, we quantify sediment transport
13 histories using cosmogenic ^{21}Ne in quartzite pebbles from modern river gravels and
14 Neogene conglomerates from the modern and ancient North Platte River of the Great
15 Plains of Nebraska. We demonstrate that at ~400 km from the Rockies mountain front,
16 the majority of pebbles must have been stored in older channel deposits for up to several
17 millions of years before being recycled; this is enabled by very slow to zero basin
18 subsidence rates. This implies that upstream tectonic or climatic controls on surface
19 processes are decoupled from the downstream depositional record; a result supported by
20 the similarities in cosmogenic ^{21}Ne between Miocene, Pliocene and modern river channel
21 pebbles despite known changes in tectonic and climatic forcing.

22 **INTRODUCTION**

23 The stratigraphic record of fluvial conglomerates far from their source area has
24 been used to interpret: 1) the timing of thrust activity (Wiltschko and Dorr, 1983), 2)
25 reduction in subsidence rates of basins adjacent to mountain ranges (Burbank et al., 1988;
26 Allen et al., 2013), and 3) climatically-forced increases in late Cenozoic global erosion
27 rates (Peizhen et al., 2001). The key to interpreting conglomerate progradation is to
28 understand how coarse river bedload generated in upland catchments is routed hundreds
29 of kilometres from mountain fronts into alluvial plains. The simplest interpretation is that
30 repeated bedload transport during seasonal bankful discharge is able to selectively
31 transport pebbles and cobbles hundreds of kilometres downstream before they are buried
32 due to regional basin subsidence (Heller and Paola, 1992). However, the storage of
33 conglomerates in paleo-channel networks and their recycling during erosion by younger
34 channels of the modern floodplain in slowly subsiding sedimentary basins (Bridge and
35 Leeder, 1979) requires longer durations of sediment routing and the progressive
36 decoupling of source to sink signals. Testing these mechanisms requires quantification of
37 the history of sediment routing including the effects of storage and recycling, which, until
38 now, has not been achievable.

39 Determining rates of landscape change has been revolutionised by the
40 measurement of in-situ cosmogenic nuclides, in particular the measurement of
41 catchment-averaged erosion rates using ^{10}Be in river sediment (Brown et al., 1995).
42 Despite the importance of sediment storage in floodplains, there have been few attempts
43 to use cosmogenic nuclides to quantify sediment transport and storage on the 10 kyr to
44 Myr time scale. Wittmann et al. (2009) and Wittman and von Blanckenburg (2009) used

45 cosmogenic ^{10}Be and $^{26}\text{Al}/^{10}\text{Be}$ ratios in bulk sand from Amazon tributaries that drain the
46 cratonic shield to argue for minimal storage and recycling.

47 The stable cosmogenic nuclides ^3He (Margerison et al. 2005) and ^{21}Ne (Ma and
48 Stuart, 2017) do not decay after production, and so their measured concentrations record
49 (minimum) surface exposure times of several million years, or erosion rates of less than
50 0.05 m/Myr. In the case of detrital material, the cosmogenic ^{21}Ne in quartz-rich pebbles
51 from rivers can be used to quantify the spatial distribution of sediment production across
52 a catchment (e.g., Codilean et al. 2008). Such studies assume that nucleogenic ^{21}Ne
53 generated over the lifetime of the rock and cosmogenic ^{21}Ne produced during transport
54 and storage of the sediment are trivial.

55 Here we report cosmogenic Ne concentrations in quartzite pebbles from the North
56 Platte River on the Great Plains of Nebraska in order to test for the influence of sediment
57 storage and recycling versus first-generation bedload transport in the routing of far-
58 traveled (~400 km) conglomerates. We show that the cosmogenic ^{21}Ne generated during
59 transport and storage on the flood plain dominates the inventory in most pebbles. The
60 bedload transport rates needed to generate the cosmogenic ^{21}Ne in modern and Neogene
61 pebbles are orders of magnitude lower than modern calculated bedload transport rates
62 requiring flood plain storage for up to several millions of years before being recycled into
63 active channels.

64 **THE GREAT PLAINS OF NEBRASKA**

65 The Great Plains east of the Rocky Mountains are dissected by east-flowing rivers
66 such as the North Platte River in Wyoming and Nebraska (Fig. 1). The stratigraphy of the
67 Great Plains records a regional unconformity separating Cretaceous strata from 50 to 250

68 m of overlying Oligocene to present-day aeolian and fluvial sediment (Condon, 2005).
69 The current high elevation of the western Great Plains (~1600 m) has been interpreted in
70 terms of increasing surface elevation driven by tectonics (Leonard, 2002; Heller et al.,
71 2003). Reconstructed channel gradients of Miocene and Pliocene North Platte paleo-
72 channels has been used to suggest hundreds of meters of surface uplift of the proximal
73 river systems between 6 and 4 Ma (Duller et al., 2012). Subsequent dissection of the
74 Great Plains by modern rivers is also interpreted in terms of climatic changes (Wobus et
75 al., 2010; Pelletier, 2009).

76 The Neogene sedimentary record of the river systems of the Great Plains records
77 several episodes of incision and aggradation (Swinehart et al., 1985). The succession
78 comprises the White River Group (late Eocene to Oligocene), the Arikaree Group
79 (Oligocene to Miocene) and the Ogallala Group (18–6 Ma). The upper Ogallala Group
80 contains the Duer Ranch beds at its base (12–10 Ma) which incise into the underlying
81 successions, and largely comprise conglomeratic channel units. Above this, the Ash
82 Hollow Formation (10–6 Ma) comprises east-west oriented gravel-rich channel bodies
83 encompassed in floodplain siltstones (Fig. 1; Diffendal, 1982). Following aggradation of
84 this fluvial system, subsequent incision and aggradation deposited the Broadwater
85 Formation between 3.7 and 2.5 Ma (Swinehart et al., 1985). Subsequent incision has
86 resulted in the formation of the ‘Rocky Flats’ terrace surface that was incised from 1 to 2
87 Ma (Riihimaki et al., 2006), resulting in the modern topography of the plains. The gravels
88 from the Ash Hollow and Broadwater Formations as well as the modern river channel
89 contain clasts derived from the Rocky Mountains including quartzite pebbles from the

90 Medicine Bow Range (Stanley, 1976; Swinehart and Diffendal, 1987) which form > 10%
91 of the populations.

92 **SAMPLES AND ANALYSIS**

93 Twenty-six, 1–6 cm pebbles of quartzite derived from the Medicine Bow
94 mountains (MBq) were sampled from the modern river channel, and ten from both
95 Pliocene and Miocene channel deposits of the Broadwater and Ash Hollow Formations
96 respectively (Supplementary Table). Sample sites are ~400 km from the mountain front,
97 and ~1050 km from the Medicine Bow Mountains along the river channel (Fig. 1). The
98 Miocene and Pliocene pebbles were selected from channel gravel bodies where the
99 samples were shielded from modern exposure to cosmic rays. Images of sample locations
100 are in Figures DR1–DR3 in the GSA Data Repository¹.

101 The non-atmospheric Ne (Ne*) in detrital quartz is largely composed of
102 nucleogenic Ne (Ne_{nuc}), generated over the lifetime of the rock, and cosmogenic Ne
103 (Ne_{cos}) generated during bedrock exhumation (Ne_{cosE}) and transport and storage in the
104 fluvial system (Ne_{cosTS}). In order to determine the Ne_{nuc} concentration, quartzite samples
105 (n = 4) were collected from the Medicine Bow Mountains from a > 12 m deep roadcut.
106 Quartz preparation and Ne isotope analysis at SUERC followed established procedures
107 (Codilean et al. 2008). The CREU quartz standard (Vermeesch et al. 2015) was analyzed
108 throughout all analytical periods as an internal check on procedures.

109 **RESULTS**

110 The shielded MBq samples from the source area have low concentrations of the
111 inherited nucleogenic ²¹Ne (0.22–0.77 × 10⁷ atoms/g) and have Ne isotope compositions
112 that plot on or near the air-spallation mixing line (Fig. DR5). These results indicate that

113 we can account for the inherited non-cosmogenic $^{21}\text{Ne}_{\text{nuc}}$, and so identify the cosmogenic
114 $^{21}\text{Ne}_{\text{cos}}$ generated in the quartzite lithology during sediment exhumation and transport.
115 Detrital sands from streams on the exposed quartzites of the Medicine Bow Mountains
116 have been used to calculate exhumation rates of bedrock based on ^{10}Be concentrations of
117 0.32×10^7 atoms $^{10}\text{Be}/\text{g}$ (Dethier et al., 2014); this represents the slowest mean
118 exhumation rates of the southern Rocky Mountains of 9 mm/kyr (Dethier et al., 2014).
119 Based on the $^{10}\text{Be}/^{21}\text{Ne}$ production rate ratio of Balco and Shuster (2009), this yields a
120 $^{21}\text{Ne}_{\text{cosE}}$ concentration of 0.08×10^7 atoms/g. Using the upper limits for both $^{21}\text{Ne}_{\text{nuc}}$ and
121 $^{21}\text{Ne}_{\text{cosE}}$, the quartzite pebbles have inherited a maximum of 0.85×10^7 atoms $^{21}\text{Ne}/\text{g}$
122 prior to downstream transport and possible storage.

123 The MBq pebbles from the modern North Platte River yield $^{21}\text{Ne}^*$ concentrations
124 of $1.1\text{--}12.6 \times 10^7$ atoms/g (Fig. 2; Table DR1). All samples plot within one standard error
125 of the air-spallation mixing, and have $^{21}\text{Ne}^*$ concentrations that are in excess of the upper
126 limit of inherited ^{21}Ne . By subtracting the inherited ^{21}Ne we obtain $^{21}\text{Ne}_{\text{cosTS}}$
127 concentrations that range from 0.25 to 11.75×10^7 at/g (Fig. 2).

128 All the MBq pebbles from Upper Miocene and Pliocene paleochannel deposits
129 yield $^{21}\text{Ne}_{\text{cosTS}}$ concentrations ranging from 0.25 to 32.0×10^7 atoms/g and $0.12\text{--}6.02 \times$
130 10^7 atoms/g respectively (Fig. 2). Although fewer Pliocene and Miocene pebbles were
131 analyzed than from modern deposits, a similar proportion (70%–80%) have $^{21}\text{Ne}_{\text{cosTS}}$
132 concentrations that are at least twice the inherited ^{21}Ne contribution.

133 The modern and ancient river systems contain pebbles with a significant variation
134 in $^{21}\text{Ne}_{\text{cosTS}}$ concentrations acquired during the ~ 1050 km of sediment transport from the
135 Medicine Bow Mountains to the sampling site. The median value of $^{21}\text{Ne}_{\text{cosTS}}$ in all three

136 stratigraphic levels lies within the 1st and 3rd quartiles of each population, and so are
137 not considered statistically distinct (Fig. 2 and supplementary Figure DR7). For the first
138 time, these results enable us to determine the duration of exposure at or near the surface,
139 and hence consider processes of sediment routing from the Miocene, Pliocene and
140 modern North Platte River.

141 **STEADY BEDLOAD TRANSPORT VERSUS STORAGE AND RECYCLING**

142 The $^{21}\text{Ne}_{\text{cosTS}}$ in the MBq pebbles records cosmic ray irradiation in the upper few
143 meters of the surface during sediment transport from the low-order tributaries of the
144 Medicine Bow Mountains into the main channel of the North Platte River and
145 downstream to the sample site. We assess whether the measured $^{21}\text{Ne}_{\text{cosTS}}$ can be
146 generated by steady bedload transport. For sediment transport during bank-full floods, the
147 highest possible concentrations are generated by slow pebble transport down the channel
148 when the pebble remains at the surface of a gravel bar following each short-lived
149 transport event. We construct a rudimentary and conservative model that assumes pebbles
150 are transported incrementally down the modern river channel, and at each step, it
151 calculates the acquisition of $^{21}\text{Ne}_{\text{cosTS}}$ based on changing production rates as a function of
152 a pebble's elevation (graphical output and details of model in Supplementary Figure
153 DR8). Production rates are determined using the Lal/Stone scaling (Lal, 1991; Stone
154 2000). This scaling scheme uses atmospheric pressure to determine production rate so we
155 follow Balco et al. (2008) and convert latitude and elevation data along the river profile
156 to pressure based on NCEP2 climate reanalysis data (Compo et al., 2011). For each run,
157 the average downstream transport rate is held constant, and pebbles are assumed to
158 always rest at the surface allowing for maximum accumulation of $^{21}\text{Ne}_{\text{cosTS}}$; in reality,

159 pebbles will be submerged beneath a depth of water, and be buried within bedforms
160 during the majority of their transport history. There is no accounting for pebble abrasion
161 which again would increase the required exposure duration for a given $^{21}\text{Ne}_{\text{cosTS}}$
162 concentration. The purpose of this scenario is to calculate the maximum possible
163 $^{21}\text{Ne}_{\text{cosTS}}$ accumulation: additional complexity in terms of sediment burial and abrasion
164 would reduce the amount of $^{21}\text{Ne}_{\text{cosTS}}$. Our conservative estimate implies minimum
165 transport time, without burial or abrasion, to accumulate enough $^{21}\text{Ne}_{\text{cosTS}}$ to account for
166 the measured concentrations.

167 The model indicates that the lowest $^{21}\text{Ne}_{\text{cosTS}}$ (0.25×10^7 atoms/g) measured in
168 the modern pebbles requires a bedload transport rate of 23 m/yr, while the average
169 concentration (2.9×10^7 atoms/g) requires an average rate of 1.9 m/yr implying >550 kyr
170 transport duration. The highest measured $^{21}\text{Ne}_{\text{cosTS}}$ concentration equates to modeled
171 bedload transport durations of >5 Myr (Fig. 2).

172 We approximate the long-term ($>10^4$ yrs) bedload transport rates for the 1050 km
173 channel reach based on a volumetric flux approach that aims at minimising the sediment
174 flux rate, and so maximising its chances of being comparable to modeled results above
175 for bedload transport. Average long-term bedrock exhumation rates of 9–31 mm/kyr are
176 recorded by ^{10}Be concentrations (Dethier et al. 2014). The upstream catchment area of
177 the North Platte River from the mountain front at the town of Douglas is 47,336 km²
178 based on the digital topography (Fig. 1). By multiplying this area by the lowest erosion
179 rate for the region (9 mm/kyr), we obtain a conservative estimate of sediment yield from
180 the catchment area of 4.3×10^5 m³/yr. The bedload proportion can be approximated at
181 between 1 and 10% (Turowski, et al., 2010). Again, taking the most conservative option

182 of 1% gives a bedload flux of $4.3 \times 10^4 \text{ m}^3/\text{yr}$. The mean cross-sectional area of the active
183 bedload in the North Platte channel can be estimated from a channel width of $\sim 100 \text{ m}$
184 from remote imagery, and an active bedload depth of 1.5 m based on documented
185 bedform height (Crowley, 1983). By dividing the volume of bedload flux by the mean
186 cross sectional area we obtain a minimum estimate for the mean bedload transport rate of
187 284 m/yr , averaged over thousands of years. Such transport rates would generate $\ll 1 \times$
188 $10^5 \text{ atoms } ^{21}\text{Ne}_{\text{cosTS}}/\text{g}$ based on the model described above. We conclude that, even
189 assuming minimum bedload transport rates with maximum source area residence times,
190 the model of steady bedload transport down an active North Platte River is unrealistic to
191 explain the measured $^{21}\text{Ne}_{\text{cosTS}}$ in the quartzite pebbles of the modern river sediment. We
192 are unable to directly model the Miocene and Pliocene channels, but it is believed that
193 they took a more direct route across the Front Ranges from the Medicine Bow Mountains
194 (Diffendal, 1982; Condon, 2005), and that their elevations were lower than they are today
195 (e.g., Duller et al., 2012). Consequently, $^{21}\text{Ne}_{\text{cosTS}}$ would have been even less than that for
196 the modern river.

197 Based on the model calculations, we propose that the high and variable $^{21}\text{Ne}_{\text{cosTS}}$
198 concentrations must record acquisition during storage in a floodplain setting on a 10^5 - 10^6
199 (and possibly 10^7) year timescale followed by reworking into active channels (Fig. 3).
200 The proximity of Miocene and Pliocene paleo-channels that run sub-parallel to the
201 modern North Platte River has been well documented (Diffendal, 1982; Condon, 2005).
202 Tributaries of the North Platte throughout the Great Plains of Nebraska and Colorado
203 drain and recycle sediment from these paleochannels (Fig. 1).

204 Our data indicate that all the sampled pebbles in the modern and ancient channels
205 of the North Platte River must have experienced periods of storage, with some for a
206 combined minimum of 5 Myr, followed by recycling back into active channels (Fig. 3).
207 This process can only take place where long-term sediment accumulation rates are slow
208 relative to lateral channel migration rates and production rates of cosmogenic nuclides.
209 This provides a mechanism by which slow basin subsidence rates facilitate long-distance
210 progradation of conglomerates into sedimentary basins (Burbank et al., 1988; Paola et al.,
211 1992; Allen et al., 2013). We conclude that in the modern and Neogene of the Great
212 Plains, recycling of gravels is a requirement for the progradation of far-traveled
213 conglomerates (Fig. 3). However, changes in water and sediment discharge or changes in
214 channel gradients since the Miocene are not reflected in these data (cf. Leonard, 2002;
215 Heller et al., 2003; Pelletier, 2009; Wobus et al., 2010; Duller et al., 2012). We conclude
216 that this is a function of the decoupling and mixing of the signals between source area
217 forcing and depositional response in these settings.

218 **CONCLUSIONS**

219 The concentration of cosmogenic ^{21}Ne in quartzite pebbles can be used to assess
220 fluvial sediment routing when inherited ^{21}Ne is constrained. In the Great Plains of
221 Nebraska, pebbles of quartzite from the Medicine Bow Mountains of Wyoming provide a
222 suitable target for understanding the sediment dynamics of the North Platte River and its
223 Miocene and Pliocene equivalents. The $^{21}\text{Ne}_{\text{cosTS}}$ content of quartzite pebbles ~400 km
224 from the mountain front is orders of magnitude higher than would be achieved by steady
225 sediment transport down the river channel. All the sampled pebbles require storage in,
226 and recycling from paleo-channels, with the highest concentrations in a pebble requiring

227 an absolute minimum of 5 Myr of storage. There is no significant difference in the
228 cosmogenic ^{21}Ne inventory recorded by Miocene, Pliocene and modern North Platte
229 River deposits. The results indicate an important decoupling and mixing of the signals
230 between source area forcing and depositional response in these settings. . This is the first
231 time that cosmogenic isotopes have been used to quantify sediment routing processes in
232 modern channels. The data from the Cenozoic deposits (although less statistically robust)
233 suggest that similar inferences are possible from ancient river channels. Future studies
234 that combine stable and radioactive cosmogenic nuclides (e.g., ^{10}Be and ^{26}Al) will enable
235 the history of sediment burial and recycling of modern sediments to be better quantified.

236 **ACKNOWLEDGMENTS**

237 McCann was funded by a NERC PhD studentship and Tao by a Chinese
238 Scholarship Counsel scholarship. Funding for analyses was supported by the SUERC
239 facilities coordinated by Stuart. Thanks to Jean Dixon and three anonymous journal
240 reviewers for helpful suggestions that guided revisions, and to James Schmitt for editing.

241 **REFERENCES CITED**

242 Allen, P.A., Armitage, J.J., Carter, A., Duller, R.A., Michael, N.A., Sinclair, H.D.,
243 Whitchurch, A.L., and Whittaker, A.C., 2013, The Qs problem: Sediment volumetric
244 balance of proximal foreland basin systems: *Sedimentology*, v. 60, p. 102–130,
245 <https://doi.org/10.1111/sed.12015>.
246 Balco, G., and Shuster, D.L., 2009, Production rate of cosmogenic ^{21}Ne in quartz
247 estimated from ^{10}Be , ^{26}Al , and ^{21}Ne concentrations in slowly eroding Antarctic
248 bedrock surfaces: *Earth and Planetary Science Letters*, v. 281, p. 48–58,
249 <https://doi.org/10.1016/j.epsl.2009.02.006>.

- 250 Balco, G., Stone, J.O., Lifton, N.A., and Dunai, T.J., 2008, A complete and easily
251 accessible means of calculating surface exposure ages or erosion rates from ^{10}Be
252 and ^{26}Al measurements: *Quaternary Geochronology*, v. 3, p. 174–195,
253 doi:<https://doi.org/10.1016/j.quageo.2007.12.001>.
- 254 Bridge, J.S., and Leeder, M.R., 1979, A simulation model of alluvial stratigraphy:
255 *Sedimentology*, v. 26, p. 617–644, [https://doi.org/10.1111/j.1365-](https://doi.org/10.1111/j.1365-3091.1979.tb00935.x)
256 [3091.1979.tb00935.x](https://doi.org/10.1111/j.1365-3091.1979.tb00935.x).
- 257 Brown, E.T., Stallard, R.F., Larsen, M.C., Raisbeck, G.M., and Yiou, F., 1995,
258 Denudation rates determined from the accumulation of in situ-produced ^{10}Be in the
259 Luquillo Experimental Forest, Puerto Rico: *Earth and Planetary Science Letters*,
260 v. 129, p. 193–202, [https://doi.org/10.1016/0012-821X\(94\)00249-X](https://doi.org/10.1016/0012-821X(94)00249-X).
- 261 Burbank, D.W., Beck, R.A., Reynolds, R.G.H., Hobbs, R., and Tahirkheli, R.A.K., 1988,
262 Thrusting and gravel progradation in foreland basins: A test of post-thrusting gravel
263 dispersal: *Geology*, v. 16, p. 1143–1146, [https://doi.org/10.1130/0091-](https://doi.org/10.1130/0091-7613(1988)016<1143:TAGPIF>2.3.CO;2)
264 [7613\(1988\)016<1143:TAGPIF>2.3.CO;2](https://doi.org/10.1130/0091-7613(1988)016<1143:TAGPIF>2.3.CO;2).
- 265 Codilean, A.T., Bishop, P., Stuart, F.M., Hoey, T.B., Fabel, D., and Freeman, S.P., 2008,
266 Single-grain cosmogenic ^{21}Ne concentrations in fluvial sediments reveal spatially
267 variable erosion rates: *Geology*, v. 36, p. 159–162,
268 <https://doi.org/10.1130/G24360A.1>.
- 269 Compo, G.P., et al., 2011, The Twentieth Century Reanalysis Project: *Quarterly Journal*
270 *of the Royal Meteorological Society*, v. 137, p. 1–28,
271 doi:<https://doi.org/10.1002/qj.776>.

- 272 Condon, S.M., 2005, Geologic studies of the Platte River, South-Central Nebraska and
273 adjacent areas—Geologic maps, subsurface study, and geologic history: U.S.
274 Geological Survey Professional Paper 1706.
- 275 Crowley, K.D., 1983, Large-scale bed configurations (macroforms), Platte River Basin,
276 Colorado and Nebraska: Primary structures and formative processes: Geological
277 Society of America Bulletin, v. 94, p. 117–133, [https://doi.org/10.1130/0016-](https://doi.org/10.1130/0016-7606(1983)94<117:LBCMPR>2.0.CO;2)
278 [7606\(1983\)94<117:LBCMPR>2.0.CO;2](https://doi.org/10.1130/0016-7606(1983)94<117:LBCMPR>2.0.CO;2).
- 279 Diffendal, R.F., 1982, Regional implications of the geology of the Ogallala Group (upper
280 Tertiary) of southwestern Morrill County, Nebraska, and adjacent areas: Geological
281 Society of America Bulletin, v. 93, p. 964–976, [https://doi.org/10.1130/0016-](https://doi.org/10.1130/0016-7606(1982)93<964:RIOTGO>2.0.CO;2)
282 [7606\(1982\)93<964:RIOTGO>2.0.CO;2](https://doi.org/10.1130/0016-7606(1982)93<964:RIOTGO>2.0.CO;2).
- 283 Duller, R.A., Whittaker, A.C., Swinehart, J.B., Armitage, J.J., Sinclair, H.D., Bair, A.,
284 and Allen, P.A., 2012, Abrupt landscape change post–6 Ma on the central Great
285 Plains, USA: *Geology*, v. 40, p. 871–874, <https://doi.org/10.1130/G32919.1>.
- 286 Dethier, D.P., Ouimet, W., Bierman, P.R., Rood, D.H., and Balco, G., 2014, Basins and
287 bedrock: Spatial variation in ¹⁰Be erosion rates and increasing relief in the southern
288 Rocky Mountains, USA: *Geology*, v. 42, p. 167–170,
289 <https://doi.org/10.1130/G34922.1>.
- 290 Heller, P.L., and Paola, C., 1992, The large-scale dynamics of grain-size variation in
291 alluvial basins, 2: Application to syntectonic conglomerate: *Basin Research*, v. 4,
292 p. 91–102, <https://doi.org/10.1111/j.1365-2117.1992.tb00146.x>.

- 293 Heller, P.L., Dueker, K., and McMillan, M.E., 2003, Post-Paleozoic alluvial gravel
294 transport as evidence of continental tilting in the US Cordillera: Geological Society
295 of America Bulletin, v. 115, p. 1122–1132, <https://doi.org/10.1130/B25219.1>.
- 296 Lal, D., 1991, Cosmic ray labeling of erosion surfaces: in situ nuclide production rates
297 and erosion models: Earth and Planetary Science Letters, v. 104, p. 424–439,
298 doi:[https://doi.org/10.1016/0012-821X\(91\)90220-C](https://doi.org/10.1016/0012-821X(91)90220-C).
- 299 Leonard, E.M., 2002, Geomorphic and tectonic forcing of late Cenozoic warping of the
300 Colorado piedmont: Geology, v. 30, p. 595–598, [https://doi.org/10.1130/0091-
301 7613\(2002\)030<0595:GATFOL>2.0.CO;2](https://doi.org/10.1130/0091-7613(2002)030<0595:GATFOL>2.0.CO;2).
- 302 Ma, Y., and Stuart, F.M., 2017, The use of *in situ* cosmogenic ^{21}Ne in for studies on long-
303 term landscape development: Acta Geochimica, v. 37, p. 310–322,
304 doi:<https://doi.org/10.1007/s11631-017-0216-9>.
- 305 Margerison, H.R., Phillips, W.M., Stuart, F.M., and Sugden, D.E., 2005, An assessment
306 of cosmogenic ^3He surface exposure dating in the Northern Dry Valleys of East
307 Antarctica: Earth and Planetary Science Letters, v. 230, p. 163–175,
308 <https://doi.org/10.1016/j.epsl.2004.11.007>.
- 309 Paola, C., Heller, P.L., and Angevine, C.L., 1992, The large-scale dynamics of grain-size
310 variation in alluvial basins, 1: Theory: Basin Research, v. 4, p. 73–90,
311 <https://doi.org/10.1111/j.1365-2117.1992.tb00145.x>.
- 312 Pelletier, J.D., 2009, The impact of snowmelt on the late Cenozoic landscape of the
313 southern Rocky Mountains, USA: GSA Today, v. 19, p. 4–11, Peizhen, Z., Molnar,
314 P., and Downs, W.R., 2001, Increased sedimentation rates and grain sizes 2–4 Myr

- 315 ago due to the influence of climate change on erosion rates: *Nature*, v. 410, p. 891–
316 897, <https://doi.org/10.1038/35073504>.
- 317 Riihimaki, C.A., Anderson, R.S., Safran, E.B., Dethier, D.P., Finkel, R.C., and Bierman,
318 P.R., 2006, Longevity and progressive abandonment of the Rocky Flats surface,
319 Front Range, Colorado: *Geomorphology*, v. 78, p. 265–278,
320 <https://doi.org/10.1016/j.geomorph.2006.01.035>.
- 321 Stanley, K.O., 1976, Sandstone petrofacies in the Cenozoic High Plains sequence, eastern
322 Wyoming and Nebraska: *Geological Society of America Bulletin*, v. 87, p. 297–309,
323 [https://doi.org/10.1130/0016-7606\(1976\)87<297:SPITCH>2.0.CO;2](https://doi.org/10.1130/0016-7606(1976)87<297:SPITCH>2.0.CO;2).
- 324 Stone, J.O., 2000, Air pressure and cosmogenic isotope production: *Journal of*
325 *Geophysical Research. Solid Earth*, v. 105, p. 23753–23759,
326 [doi:https://doi.org/10.1029/2000JB900181](https://doi.org/10.1029/2000JB900181).
- 327 Swinehart, J.B., Souders, V.L., DeGrew, H.M., and Diffendal, R.F., Jr., 1985, Cenozoic
328 paleogeography of western Nebraska, *in* Flores, R.M., and Kaplan, S.S., eds.,
329 *Cenozoic Paleogeography of the West-Central United States: Denver, Colorado,*
330 *Society of Economic Paleontologists and Mineralogists, Rocky Mountain Section,*
331 *Rocky Mountain Paleogeography Symposium*, v. 3, p. 209–229.
- 332 Swinehart, J.B., and Diffendal Jr., R.F., 1987, Duer Ranch, Morrill County, Nebraska:
333 Contrast between Cenozoic fluvial and eolian deposition: *Geological Society of*
334 *America Centennial Field Guide—North-Central Section Trip 5*, p. 23–28.
- 335 Turowski, J.M., Rickenmann, D., and Dadson, S.J., 2010, The partitioning of the total
336 sediment load of a river into suspended load and bedload: A review of empirical

- 337 data: *Sedimentology*, v. 57, p. 1126–1146, <https://doi.org/10.1111/j.1365->
338 3091.2009.01140.x.
- 339 Vermeesch, P., et al., 2015, Interlaboratory comparison of cosmogenic ^{21}Ne in quartz:
340 *Quaternary Geochronology*, v. 26, p. 20–28,
341 <https://doi.org/10.1016/j.quageo.2012.11.009>.
- 342 Wittmann, H., and Von Blanckenburg, F., 2009, Cosmogenic nuclide budgeting of
343 floodplain sediment transfer: *Geomorphology*, v. 109, p. 246–256,
344 <https://doi.org/10.1016/j.geomorph.2009.03.006>.
- 345 Wittmann, H., Von Blanckenburg, F., Guyot, J.L., Maurice, L., and Kubik, P.W., 2009,
346 From source to sink: Preserving the cosmogenic ^{10}Be -derived denudation rate signal
347 of the Bolivian Andes in sediment of the Beni and Mamoré foreland basins: *Earth*
348 and *Planetary Science Letters*, v. 288, p. 463–474,
349 <https://doi.org/10.1016/j.epsl.2009.10.008>.
- 350 Wiltschko, D.V., and Dorr, J.A., Jr., 1983, Timing of deformation in overthrust belt and
351 foreland of Idaho, Wyoming, and Utah: *American Association of Petroleum*
352 *Geologists Bulletin*, v. 67, p. 1304–1322.
- 353 Wobus, C.W., Tucker, G.E., and Anderson, R.S., 2010, Does climate change create
354 distinctive patterns of landscape incision?: *Journal of Geophysical Research. Earth*
355 *Surface*, v. 115, p. F04008, doi:10.1029/2009JF001562.

356

357 **FIGURE CAPTIONS**

358

359 Figure 1. Geological map showing the location of the North Platte River in the context of
360 the Mississippi river system (A) and in its geological context with sample locations (B).
361 Note that the modern North Platte River cross-cuts the Miocene (purple dashed) and
362 Pliocene (blue dashed) paleochannels from Condon (2005). The grey outline is the
363 modern drainage divide for the North Platte River, shading outside the modern catchment
364 is in a lighter tone (see key).

365

366 Figure 2. Cumulative frequency diagram of cosmogenic $^{21}\text{Ne}_{\text{cosTS}}$ concentrations
367 generated during sediment transport and storage in modern, Pliocene and Miocene
368 quartzite pebbles sourced from the Medicine Bow Mountains sampled from the North
369 Platte River, Nebraska (Fig. 1). Top axis equates to modeled minimum transport
370 durations for pebbles sourced in the Medicine Bow Mountains and transported to the
371 sample site in the plains. The highest concentration measured in a Miocene pebble
372 equates to significantly greater than 5 Myr from source to sink.

373

374 Figure 3. Cartoon illustrating the process of the recycling of pebbles during the
375 progradation of conglomerates over alluvial plains. Red arrows illustrate the transfer of
376 ^{21}Ne -rich pebbles from abandoned channel-fills into an active channel. Graph represents
377 the production rate as a function of depth in the Plains. The total measured $^{21}\text{Ne}^*$
378 combines $^{21}\text{Ne}_{\text{nuc}}$, $^{21}\text{Ne}_{\text{cosE}}$ and $^{21}\text{Ne}_{\text{cosTS}}$.

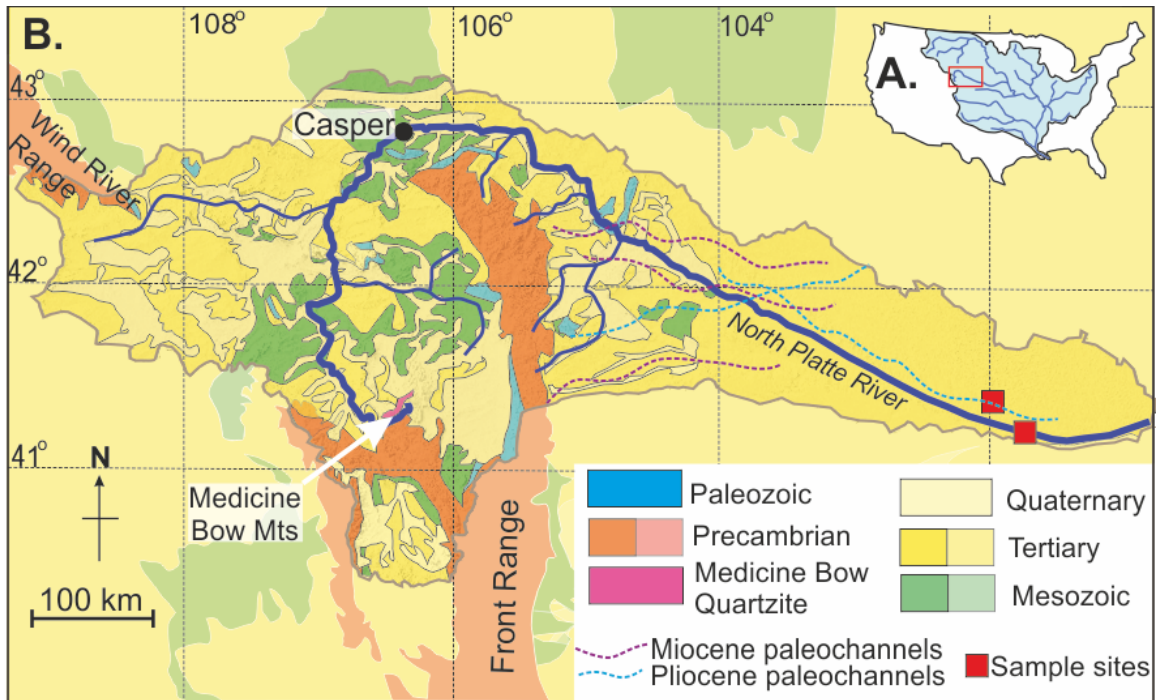
379

380 1GSA Data Repository item 2018xxx, xxxxxxxxxxxxxxxxxx, is available online at

381 <http://www.geosociety.org/datarepository/2018/>, or on request from

382 editing@geosociety.org.

383



384

385 Figure 1. Geological map showing the location of the North Platte River in the context of
386 the Mississippi river system (A) and in its geological context with sample locations (B).

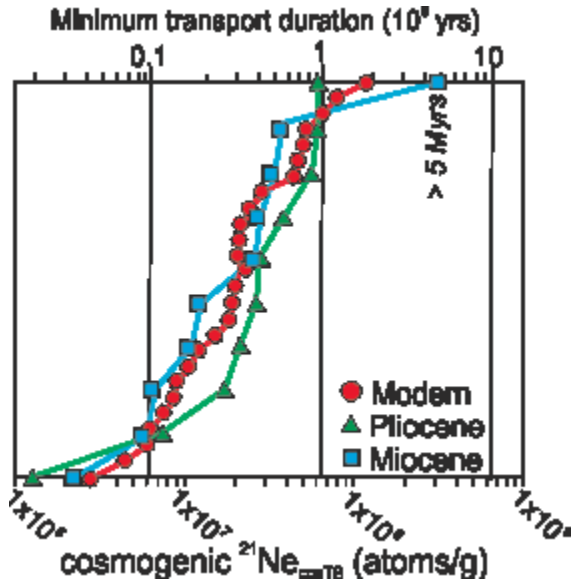
387 Note that the modern North Platte River cross-cuts the Miocene (purple dashed) and

388 Pliocene (blue dashed) paleochannels from Condon (2005). The grey outline is the

389 modern drainage divide for the North Platte River, shading outside the modern catchment

390 is in a lighter tone (see key).

391



392

393 Figure 2. Cumulative frequency diagram of cosmogenic ²¹Ne_{cosTS} concentrations
394 generated during sediment transport and storage in modern, Pliocene and Miocene
395 quartzite pebbles sourced from the Medicine Bow Mountains sampled from the North
396 Platte River, Nebraska (Fig. 1). Top axis equates to modeled minimum transport
397 durations for pebbles sourced in the Medicine Bow Mountains and transported to the
398 sample site in the plains. The highest concentration measured in a Miocene pebble
399 equates to significantly greater than 5 Myr from source to sink.

400

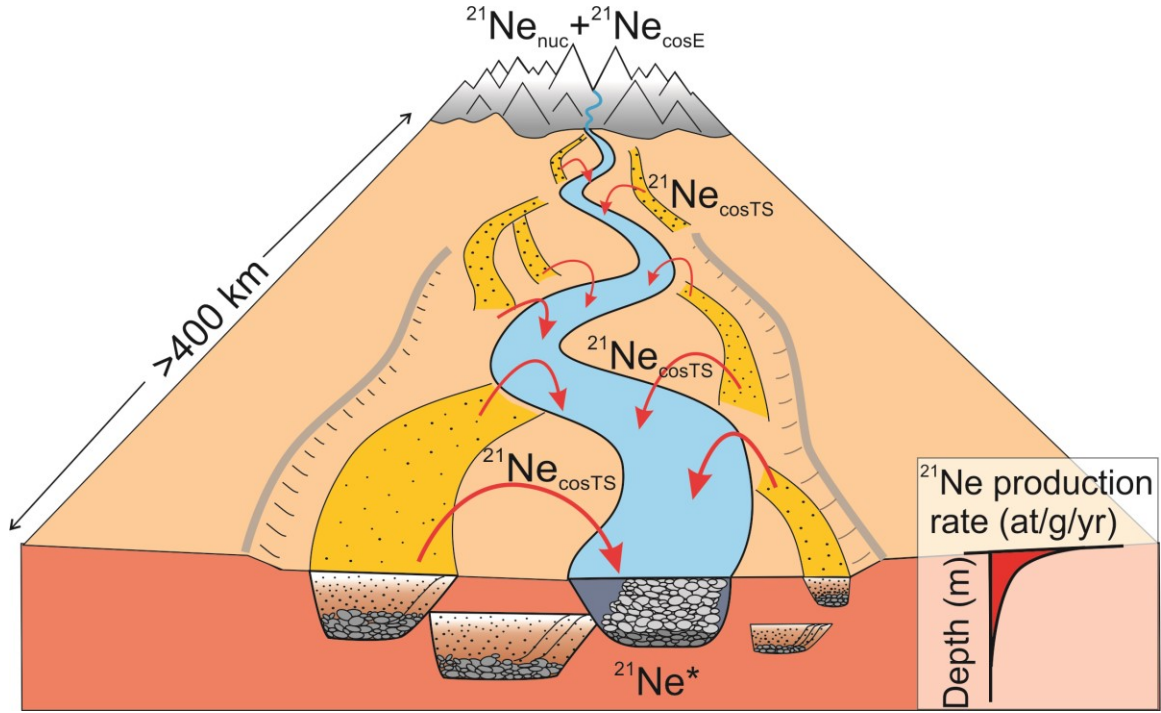


Figure 3. Cartoon illustrating the process of the recycling of pebbles during the progradation of conglomerates over alluvial plains. Red arrows illustrate the transfer of ^{21}Ne -rich pebbles from abandoned channel-fills into an active channel. Graph represents the production rate as a function of depth in the Plains. The total measured $^{21}\text{Ne}^*$ combines $^{21}\text{Ne}_{\text{nuc}}$, $^{21}\text{Ne}_{\text{cosE}}$ and $^{21}\text{Ne}_{\text{cosTS}}$.